Laser and Particle Beams (2008), *26*, 379–387. Printed in the USA.

doi:10.1017/S0263034608000396

Self-focusing effect in Au-target induced by high power pulsed laser at PALS

L. TORRISI,[1,2] D. MARGARONE,[1,2] L. LASKA,[3] J. KRASA,[3] A. VELYHAN,[3] M. PFEIFER,[3] J. ULLSCHMIED,[3] AND L. RYC[4]

[1]Dipartimento di Fisica, Università di Messina, Messina, Italy
[2]INFN-Laboratori Nazionali del Sud, Catania, Italy
[3]Institute of Physics, ASCR, Prague, Czech Republic
[4]Institute of Plasma Physics and Laser Microfusion, Warsaw, Poland

(Received 20 December 2007; Accepted 26 May 2008)

Abstract

Self-focusing effects, induced by ASTERIX pulsed laser at PALS Laboratory of Prague, have been investigated. Laser was employed at the third harmonics (438 nm) and intensities of the order of 10^{16} W/cm^2. Pure Au was used as thin target and irradiated with 30° incidence angle. An ion energy analyzer was employed to detect the energy-to-mass ratio of emitted ions from plasma. Measurements were performed by changing the focal point position with a high spatial resolution step-motor. Results demonstrated that non linear processes, due to self-focusing effects, occurs when the laser beam is focused at about 200 μm in front of the target surface. In such conditions, a new ion group, having high charge state and kinetic energy, is produced because of the increment in temperature of the laser-generated plasma.

Keywords: Laser focalization; Laser-generated plasma; Plasma temperature; Plasma density; Self-focusing

1. INTRODUCTION

The production of ions with high intensity, charge state, and kinetic energy, by using power pulsed lasers is assuming more and more importance in many application fields (nuclear fusion, laser ion source, new generation ion accelerators, ion implantation, etc.) (Laska *et al.*, 2007; Malka & Fritzler, 2004; Lifschitz *et al.*, 2006; Mangles *et al.*, 2006; Batani *et al.*, 2007; Koyama *et al.*, 2006).

Highly charged heavy ions can be obtained by ps and ns high power pulsed laser irradiating heavy elements (Laska *et al.*, 2004). The electronic temperature of the laser-generated plasma, the average charge state, and the mean ion energy increase with the laser intensity.

Many experiments regarding the generation of highly charged ions are currently accompanied by the laser interaction with preformed plasma. Preformed plasma can be produced by a separate laser pre-pulse preceding the main laser pulse (Laska *et al.*, 2005*a*, 2007). However, even the main pulse itself significantly participates in the pre-plasma formation, in fact, self-created pre-plasma is formed from the front part of the long laser pulses or due to the long lasting intensity background of the short pulses (Laska *et al.*, 2006*a*).

The interaction of the laser radiation above some threshold intensity with a plasma of defined properties may significantly increase the charge state and energy of the produced ions, due to a peculiar effect occurring in the plasma, which focalizes further the laser pulse (self-focusing effect) acting so as a small vapor lens placed in front of the target surface. Advances in laser technology have recently enabled the observation of self-focusing in the interaction of intense laser pulses with plasmas. Self-focusing in plasma can occur through thermal, relativistic, and ponderomotive effects (Giulietti & Gizzi, 1998; Giulietti *et al.*, 2007; Laska *et al.*, 2006*b*).

Thermal self-focusing is due to collisional heating of plasma exposed to electromagnetic radiation: the rise in temperature induces a hydrodynamic expansion, which leads to an increase of the refraction index and further heating. Relativistic self-focusing is caused by the mass increase of electrons traveling at speed approaching the speed of light, which modifies the plasma refractive index, depending on the electromagnetic and plasma frequencies. Ponderomotive self-focusing is caused by the ponderomotive

Address correspondence and reprint requests to: L. Torrisi, INFN-Laboratori Nazionali del Sud, Via S. Sofia 62, 95125 Catania, Italy. E-mail: torrisi@lns.infn.it

force, which pushes electrons away from the region where the laser beam is more intense, therefore increasing the refractive index and inducing a focusing effect.

The evaluation of the contribution and interplay of these processes is a complex task, but a reference threshold for plasma self-focusing is the relativistic critical power which must be reached (Sun *et al.*, 1987):

$$P_{cr}(GW) = \frac{m_e c^5 \omega^2}{e^2 \omega_p^2} \cong 17\left(\frac{\omega}{\omega_p}\right)^2, \quad (1)$$

where m_e is the electron mass, c is the speed of light, ω is the radiation angular frequency, e is the electron charge, and ω_p is the plasma frequency. This last quantity depends on the relationship (Sun *et al.*, 1987):

$$\omega_p(rad/s) = \sqrt{\frac{n \cdot e^2}{m_e \varepsilon_0}}, \quad (2)$$

where n is the electron density and ε_o is the permittivity in vacuum.

For an electron density of 10^{19} cm^{-3} and radiation at the wavelength of 438 nm, the critical power is about 980 GW, lower with respect to the maximum PALS laser power of the order of 10^{13} W.

Self-focusing in plasma can balance the natural diffraction and channel a laser beam. Such effect is beneficial for many applications, since it helps increasing the length of the interaction between laser and medium. This is crucial, for example, in laser-driven particle acceleration, laser-fusion schemes and high harmonic generation (Malka & Fritzler, 2004; Malka *et al.*, 2006; Lifschitz *et al.*, 2006; Mangles *et al.*, 2006). Self-focusing effects are obtained overall by using pico-second and femto-second lasers with intensities higher than 2×10^{14} W/cm^2, which induce particularly the evidence for the phenomenon because they induce a net increment of the average charge state and ion energy of the plasma (Sun *et al.*, 1987). In this contribution, the laser generation of Au ions with the highest charge states and the highest energy was studied using long pulse of the PALS iodine laser at the third harmonic frequency, and changing the laser focus positions.

2. MATERIALS AND METHODS

Experiments were performed with the high-power iodine laser system at the PALS Research Center ASCR in Prague, operating at a maximum pulse energy of 1 kJ, a pulse duration of 300 ps, and 1.315 μm fundamental frequency (Jungwirth, 2005; Batani *et al.*, 2007). All presented results were obtained irradiating in vacuum (10^{-6} mbar) Au thin targets (500 μm thick) with the third harmonic (3ω), at 438 nm wavelength, and with laser pulse energy of 150 J.

The ion diagnostics was based mainly in an ion collector ring (ICR) and an electrostatic ion energy analyzer (IEA) useful for online monitor of the ion emission from plasma and to measure the energy-to-charge ratio. Time-of-flight (TOF) technique was employed to measure the arrival time of the ion signal and the corresponding ion velocity and energy. Both ICR and IEA were situated in the far expansion zone of the plasma, orthogonal to the target surface, and at a distance of 190 cm and 262 cm, respectively.

The laser beam was focused on the flat surface of the pure Au target, which was irradiated, with an incidence angle of 30°. The bias of the IEA deflection plates was maintained constant at ±1500 V, i.e., the ratio E/z was maintained constant at 30 keV/charge state (Woryna *et al.*, 1996). The focal position (FP) of the focusing lens has been changed, gradually, in the range $-1500\ \mu m \leq FP \leq +1500\ \mu m$ by means of a step motor with a resolution of ±1 μm. The convention used is that FP = 0 when minimum focal spot coincides with the target surface, while FP < 0 means that the minimum focal spot is located in front of the target surface, and FP > 0 means that it is inside the target, as shown in Figure 1.

The laser intensity (I_L) is calculable knowing the pulse energy (E_L), the spot area on the target surface (S), and the pulse duration (Δt):

$$I_L(W/cm^2) = \frac{E_L}{S \cdot \Delta t}. \quad (3)$$

The spot size diameter is measurable *in-situ*, by using a suitable optical microscope, and *ex-situ* with a surface profiler (Tencor P-10) giving the crater diameter, and the crater depth profile (Torrisi *et al.*, 2002).

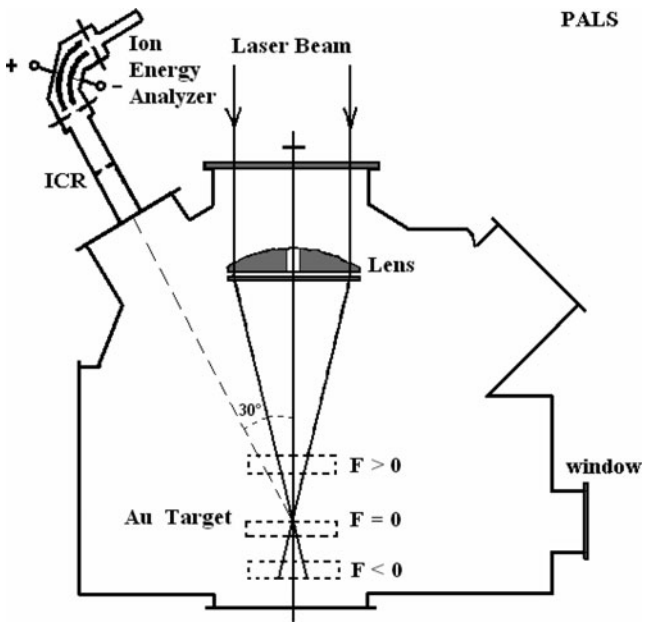

Fig. 1. Experimental set-up at PALS laboratory.

https://doi.org/10.1017/S0263034608000396 Published online by Cambridge University Press

The electronic temperature (T_e) of the non-equilibrium plasma was obtained from the theoretical approach (Giulietti & Gizzi, 1998):

$$T_e(keV) = 6 \cdot 10^{-5}[I_L(W/\mathrm{cm}^2) \cdot \lambda^2(\mu\mathrm{m}^2)]^{1/3}, \quad (4)$$

where I_L and λ are the laser intensity and laser wavelength, respectively.

The minimum spot size diameter, measured at FP = 0 μm, was 70 μm, at which corresponds to a laser intensity of 1.3×10^{16} W/cm^2 and, from Eq. (4), an electronic temperature of 8.14 keV.

3. RESULTS

Figure 2 shows three typical ion collector spectra acquired using 150 J laser pulse energy for FP = −1500 μm (a), FP = −700 μm (b), and FP = −200 μm (c), which corresponds to spot sizes 46.6×10^{-4}, 12.6×10^{-4}, and 1.8×10^{-4} cm^2, respectively. The spectra indicate that two ion groups are evident at high and low spot size, i.e., at low and high laser intensity, respectively. The first group contains fast ions (TOF < 2 μs) and the second group contains slow ions (TOF > 2 μs), respectively. The first group is generated by high charge states while the second one by low charge states, as demonstrated by contemporary IEA measurements

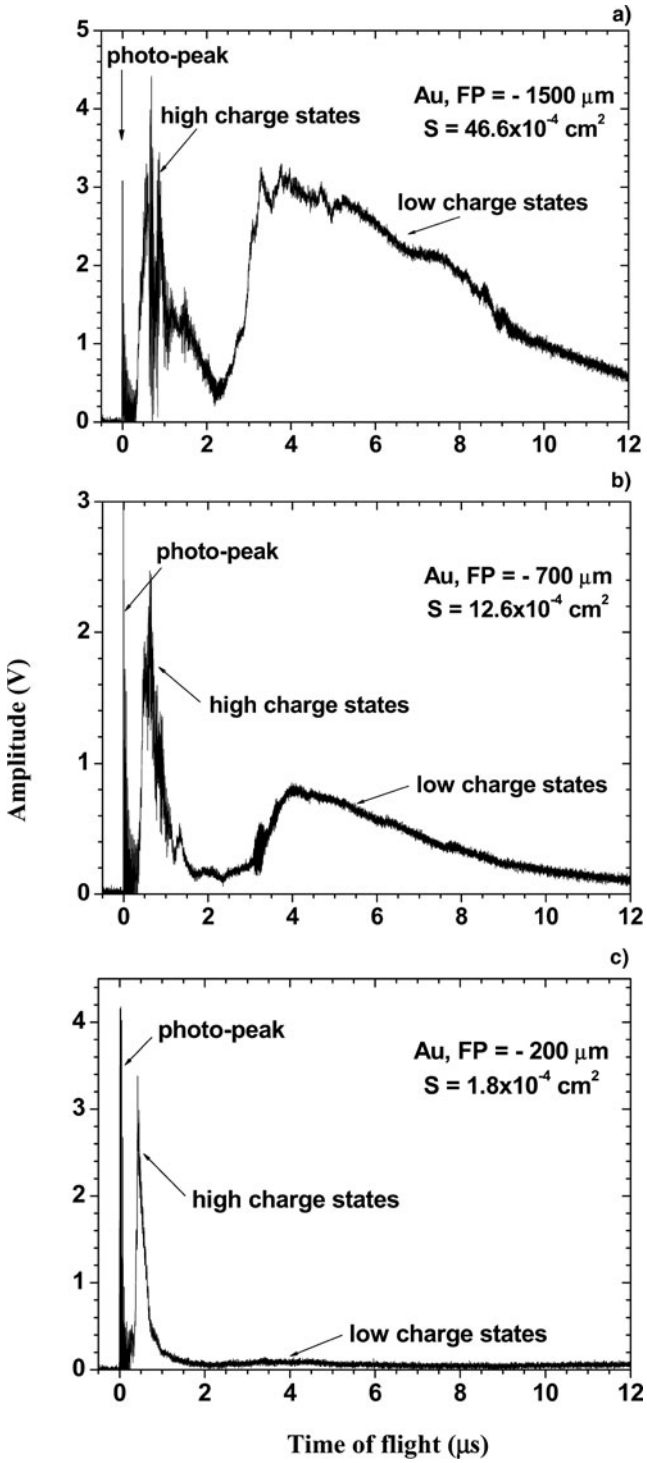

Fig. 2. ICR spectra comparison at three different focal positions: FP = −1500 μm (**a**), FP = −700 μm (**b**), and FP = −200 μm (**c**).

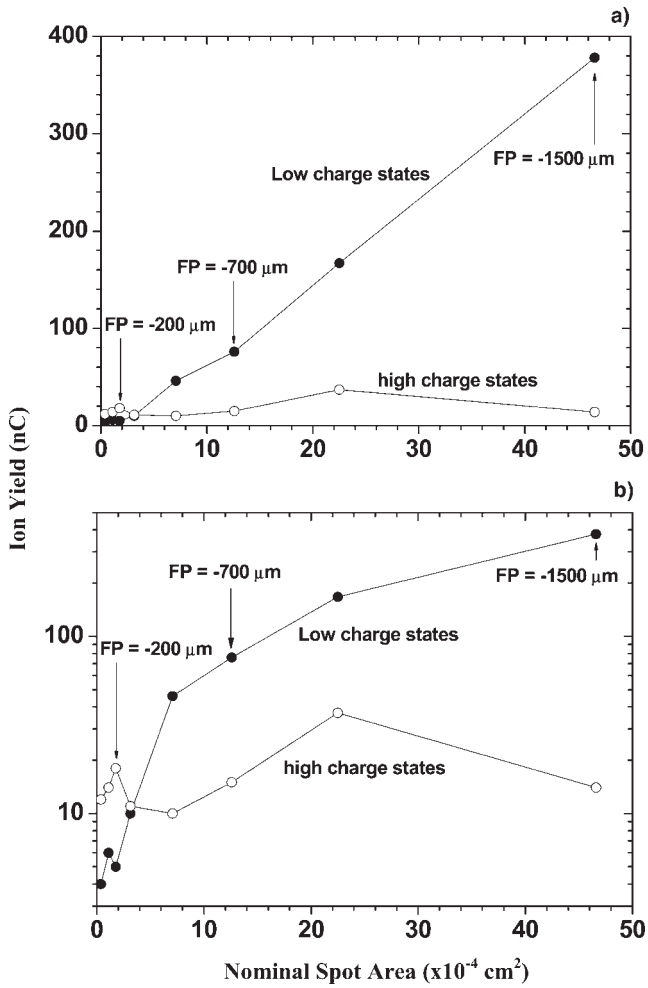

Fig. 3. Ion yield vs. nominal spot area for low and high charge states in linear (**a**) and semi-logarithmic (**b**) plots.

https://doi.org/10.1017/S0263034608000396 Published online by Cambridge University Press

of ion charge states reported below. The mean amplitude, yield, width and time of the TOF peak, for the two ion groups, depend on the used value of the focal position FP.

The ion collector measurements of the emitted slow group versus the nominal spot size, performed with the ICR placed along the normal to the target surface, indicate that the ion emission increases linearly with the spot size, except for spots lower than 2×10^{-4} cm^2, i.e., $-200\ \mu m < FP < 0$, as reported in Figure 3a. Improving the laser beam focalization, i.e., reducing the spot size, the signal amplitude of the peak due to low charge states contribution decreases, while the laser intensity and the plasma electron temperature increase.

A different effect characterizes the fast ion group. The ion collector amplitude signal of the emitted fast group versus the spot size, performed with the ICR placed along the normal to the target surface, indicates that the ion emission is independent of the spot size. At the nominal spot size of 1.8×10^{-4} cm^2 the fast component shows a peak, as evident from the semi-logarithmic plot reported in Figure 3b.

Thus, at large spot sizes, the ion current is due mainly to the slow and low charge ion group while at little spot sizes, lower than that 3×10^{-4} cm^2, the ion current is due mainly to the fast and high charge ion group.

The two detected ion groups are evident also from the IEA spectra. Figure 4 shows a typical IEA-TOF spectrum comparison registered at different focus positions during the Au target irradiation. The faster peak is due to hydrogen ions as contaminant of the Au target. The spectrum obtained at FP $= +500\ \mu m$ (a) shows only low charge states group for Au ions, from 1^+ up to 6^+, due to the large distance from the best nominal focus position (FP $= 0$). Because at this distance the laser spot is large, the corresponding laser intensity and the electronic plasma temperature are low and the ionization is minimal.

The IEA signal at FP $= 0$ (b) shows two different ion groups, probably attributable to two main ionization mechanisms occurring in the plasma, i.e., the inverse bremsstrahlung and the resonant absorption (Bell, 1996). The first group includes slower Au ions with charge states between 16^+ and 35^+, while the second one includes faster Au ions with charge states between 36^+ and 51^+. Moreover, this spectrum indicates that the yield of the fast ion group, at higher charge states, is about a factor of three higher with respect to that of the slow ion group, at lower charge states. This result indicates that at this focal position, the laser intensity is high, and that the resonant absorption mechanism, responsible for the higher charge state

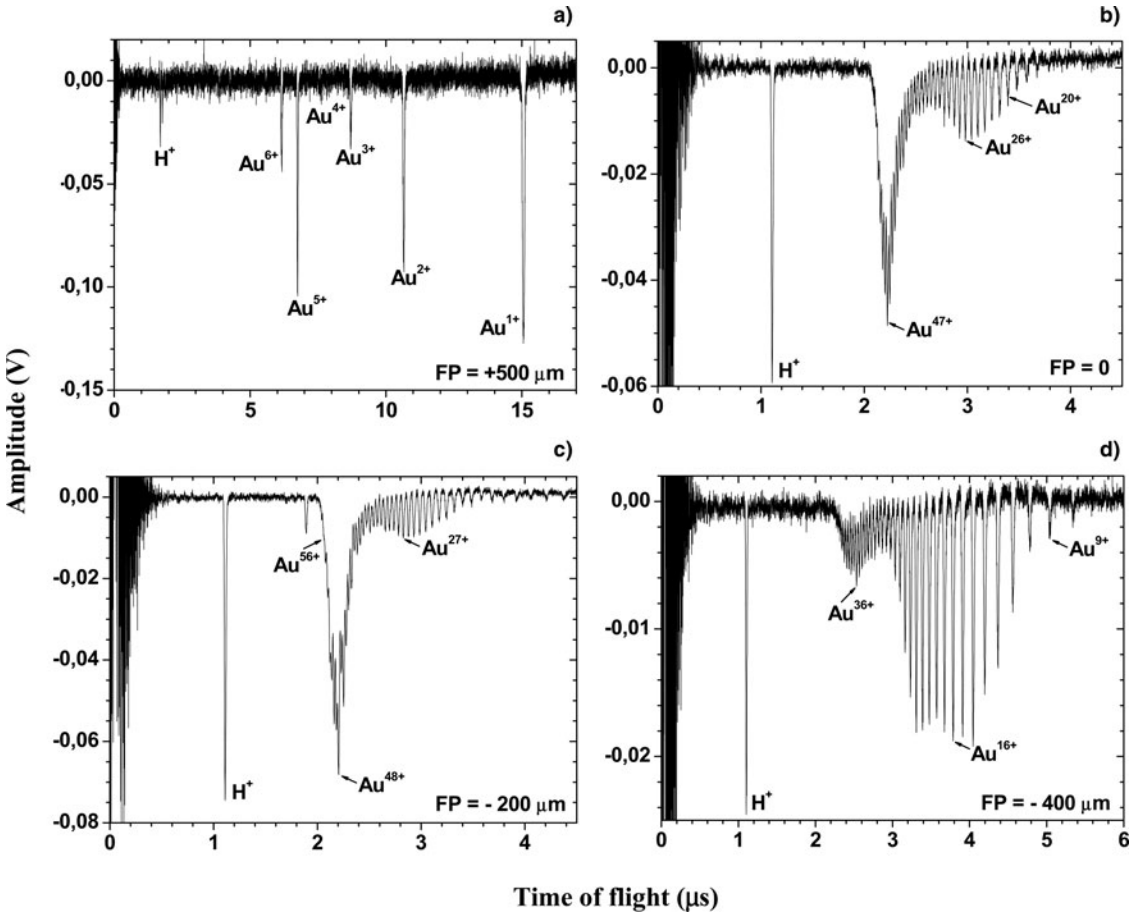

Fig. 4. IEA spectra comparison at four different focal positions: FP $= +500\ \mu m$ (**a**), FP $= 0\ \mu m$ (**b**), FP $= -200\ \mu m$ (**c**) and FP $= -400\ \mu m$ (**d**).

https://doi.org/10.1017/S0263034608000396 Published online by Cambridge University Press

formation, is predominant. In these conditions of best nominal focus position, it is not possible to distinguish the lowest charge states, from 1^+ to 15^+, due to the high laser intensity that permits to strip about 16 electrons from the plasma atoms, indicating that the laser spot is small and the corresponding laser intensity and electronic temperature high.

The TOF spectrum obtained at FP $= -200$ μm (c) is again constituted of two ion groups, where the slow one includes charge states between 10^+ and 35^+, while the fast one includes charge states between 36^+ and 56^+. Two important results have been obtained for this negative focus position: the highest charge state for Au ions (56^+) and the highest amount of the fast ion group (about a factor of six higher than the slow ion group). Both results are correlated to the overcoming of the minimal threshold of self-focusing process appearance (typically about 2×10^{14} W/cm^2 (Sun *et al.*, 1987)) produced by the very intense laser beam with the preformed plasma, which find a maximum effect when it is focused before the target surface (FP < 0) and at 200 μm distance.

Increasing further the focal position distance from the target surface (defocusing in front of the target), the charge state distribution shows a decrement. The spectrum reported in (d) was obtained for FP $= -400$ μm at which it is possible to distinguish two different ion groups and, as expected, the slower one ($Au^{8+} \div Au^{29+}$) becomes higher with respect to the faster one ($Au^{30+} \div Au^{44+}$), due to the spot increase, i.e., to the corresponding decrease in laser intensity and temperature.

Measurements demonstrated that although the minimum spot size diameter (70 μm) corresponds to a laser intensity of 1.3×10^{16} W/cm^2 and an electronic temperature of 8.14 keV, when FP $= -200$ μm is chosen, due to the self-focusing effect, a sort of further laser beam focalization reduces subsequently the laser spot diameter on the target surface, increasing the laser intensity, and the electronic plasma temperature and producing an ionization of high charge states.

In order to show the self-focusing effect, some IEA measurements of ion yield for specific ion charge states were plot reported as a function of the focus position. Figure 5 shows typical results of amplitude of Au ion signals versus focal position obtained using the IEA analyzer.

It is evident that the shape of the plots changes with the considered charge states. The amplitude of Au^{7+} and Au^{8+} signals, for example, presents a broad minimum for -500 μm $<$ FP $< +100$ μm (centered at FP $= -200$ μm) and two pronounced lateral maxima for FP $> +100$ μm and FP < -500 μm. Thus the lower charge state group is

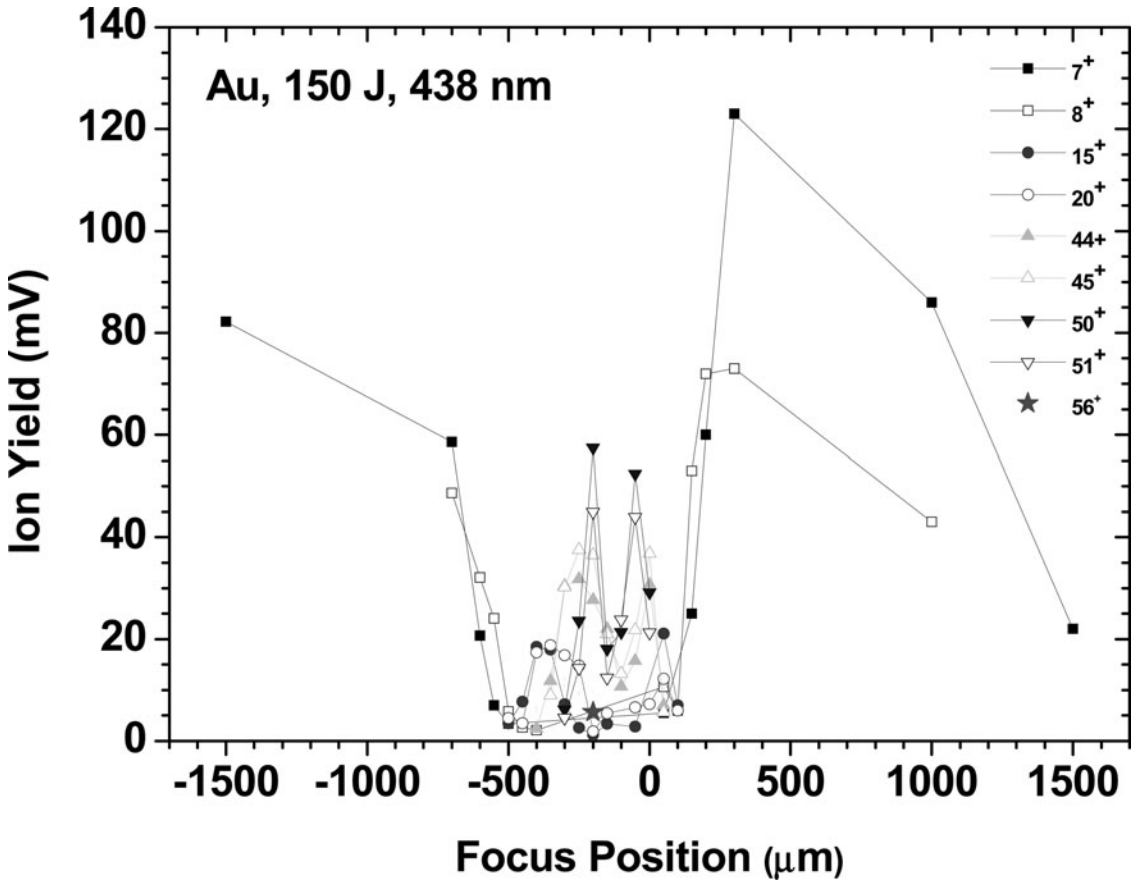

Fig. 5. Ion yield versus focal position for different charge states from Au^{7+} to Au^{56+}.

https://doi.org/10.1017/S0263034608000396 Published online by Cambridge University Press

negligible around the minimum focal spot position of FP = −200 μm. A similar behavior is shown for Au^{15+} and Au^{20+} but in this case, the minimum is narrower (−300 μm < FP < −50 μm) and it is not possible to distinguish ion signals for FP < −500 μm and FP > +100 μm.

The higher charge state signals have a complementary behavior. From Au^{44+} to Au^{56+} yields, in fact, the ion yields have a maximum peak at FP = −200 μm instead of the minimum obtained for lower charge states, moreover no ion signals are detected for FP < −400 μm and FP > +50 μm. The maximum detected charge state was Au^{56+}, surprisingly reached at FP = −200 μm (experimental best focus position) instead that FP = 0 (nominal best focus position).

The presented dependencies demonstrate an asymmetry with respect to the FP = 0 position (nominal maximum of laser intensity), in agreement with literature concerning the laser-plasma generation of highly charged ions (Laska *et al.*, 2006*b*). This effect is due to the nonlinear phenomena (both relativistic and charge displacement) related to the interaction of the intense laser beam with the preformed plasma, leading to a spatial confined (channeled) propagation of the electromagnetic wave. The self-focusing of the laser beam is considered to shrink the laser beam diameter down to the laser wavelength and increase the local laser intensity up to 10^{19} W/cm^2 (Laska *et al.*, 2004, 2006*b*). The duration of the laser-beam interaction with the expanding plasma plume influences the highest charge state and the kinetic energy of emitted ions, as well as the composition of the expanding plasma. For this reason, the highest charge state, that in principle should be detected at FP = 0, is reached at FP = −200 μm (best focus position due to self-focusing effect), i.e. there is a shift towards the lower FP < 0 positions.

Fig. 6 shows the calculated laser pulse intensity on the target surface (a) and the electronic plasma temperature (b) vs. the focus position for not-self-focusing and self-focusing conditions. The calculation of the nominal laser intensity has been performed by using Eq. (3). The spot diameter obtained at low laser energy, in not-self-focusing conditions, was measured through optical microscopy of the target surface craters for different focal positions. The used approximation to calculate the spot diameter at high laser energy, in self-focusing conditions, will be discussed in the next section. Self-focusing effect increments the maximum intensity of about 100% with respect to not self-focusing. Moreover self-focusing increments the maximum electronic temperature of about 25% with respect to the not-self-focusing conditions, justifying the higher charge states and kinetic energies of detected ions along the normal to the target surface.

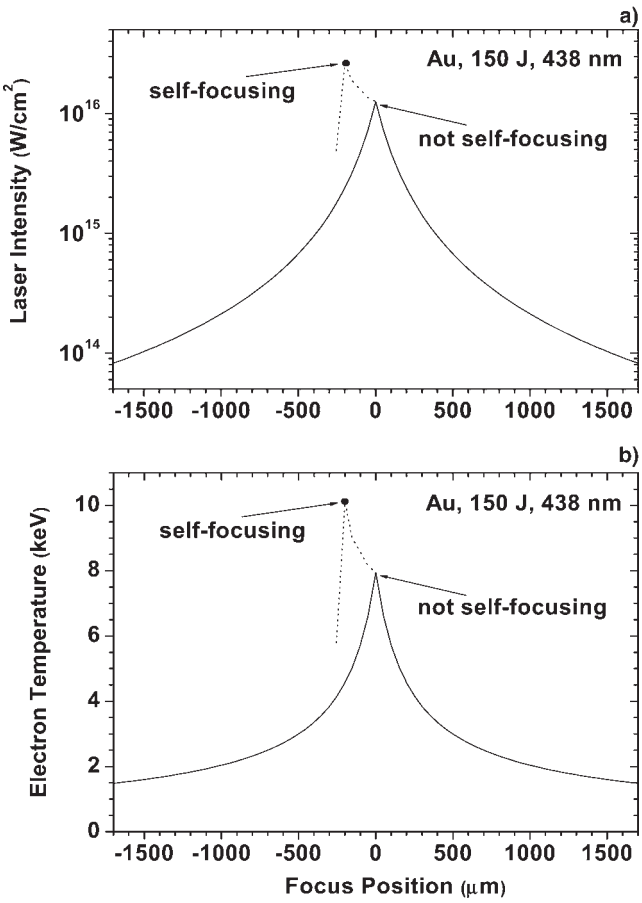

Fig. 6. Calculated laser intensity (**a**) and plasma electron temperature (**b**) versus focal position for self-focusing and not self-focusing conditions.

4. DISCUSSION AND CONCLUSIONS

The ion yield versus focus position plot of Figure 5 indicates that for low charge states, two main maxima occurs for FP < −500 μm and FP > 200 μm, and a minimum occurs for −500 μm < FP < 200 μm. These low charge state ions are due to ionization by thermal electrons generated by inverse bremsstrahlung mechanism. Such a result was ascribed to the volume effect of produced plasma due to the interaction of continuously decreasing diameter of the laser beam with respect to the target surface that, in the case of self-focusing mechanisms, is found to a forward negative focus positions, FP = −200 μm, instead that at FP = 0.

In contrast, ions with higher charge states, connected with the presence of fast electrons, and generated by resonant absorption mechanism, create a maximum yield of FP = −200 μm. The inverse bremsstrahlung prevails for both the lateral maxima, which $I\lambda^2 < 10^{15}$ W μm^2/cm^2, while the maximum yield of FP = −200 μm is related to the resonant absorption process, which $I\lambda^2 > 10^{15}$ W μm^2/cm^2 (Margarone *et al.*, 2007).

The initial laser beam diameter of 29 cm, focused by an aspheric lens (f = 600 mm for 3ω), reaches a minimum diameter value of 70 μm at FP = 0. When the focal position is FP = −200 μm and the laser energy is very low, the self-focusing cannot happen because the conditions are below the threshold value of Eq. (1) being the measured nominal spot diameter on the target surface about 160 μm, due to the laser beam divergence in

https://doi.org/10.1017/S0263034608000396 Published online by Cambridge University Press

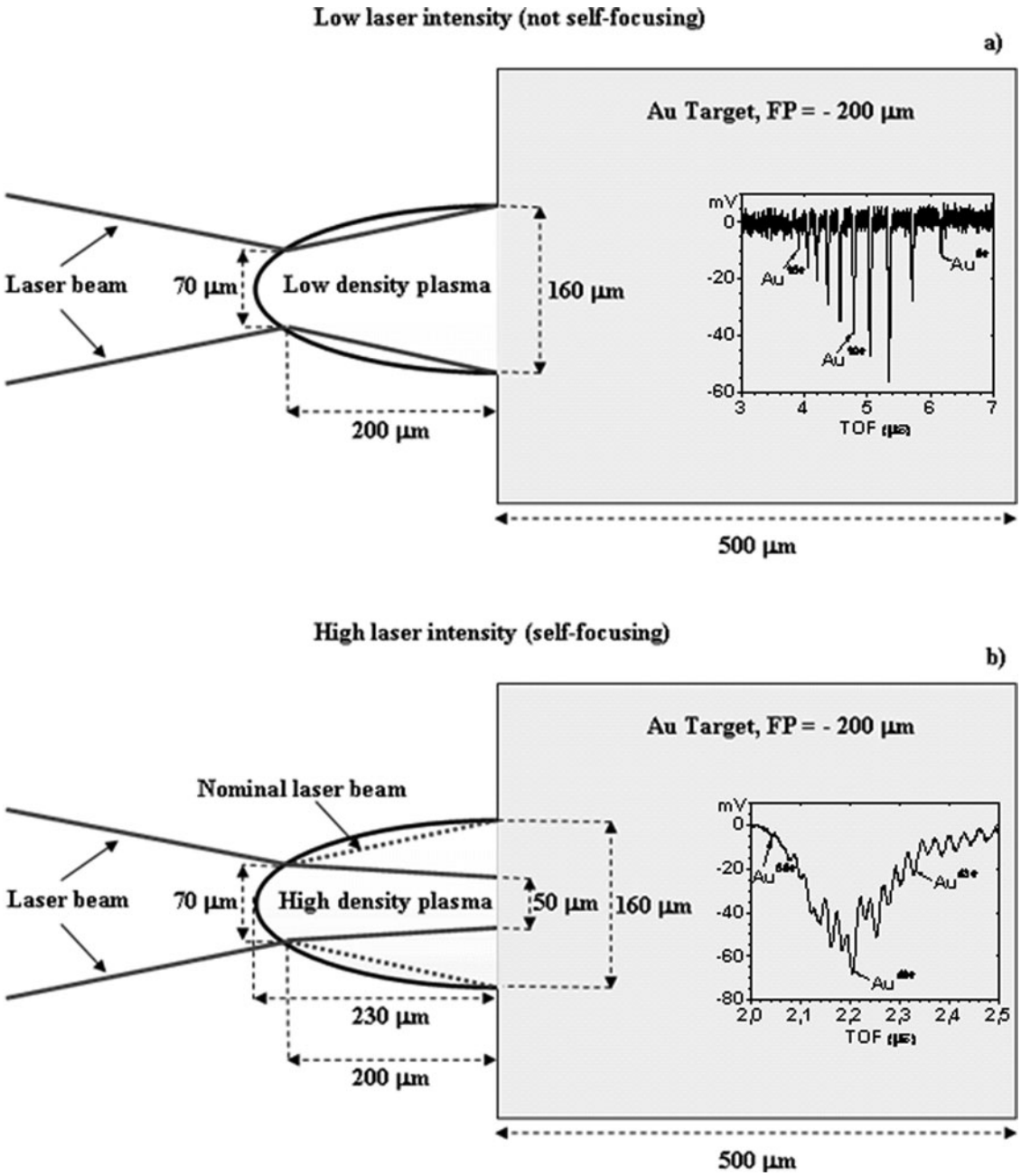

Fig. 7. Schemes of the plasma dimension developed in front of the target in condition of not self-focusing (**a**) and self-focusing (**b**).

the region $-200\ \mu m < FP < 0\ \mu m$, as reported in the scheme of Figure 7a. When the focal position is $FP = -200\ \mu m$ and the laser intensity is above the self-focusing threshold, the high light refraction effect produces a further laser beam focalization, due to the dense plasma volume in front of the target, which converges the beam so as a focusing lens. This focusing produces a laser spot diameter on the target lower than 70 μm, as depicted in the sketch of the plasma lens in Figure 7b. Such convergent plasma lens permits to reach a smaller diameter on the target surface and, as a consequence, the maximum laser intensity is not reached at $FP = 0$ (minimum nominal diameter) but at $FP = -200\ \mu m$ (best self-focusing position). Thus, the first part of the relative long pulse width (300 ps) is responsible of the formation of a pre-plasma with an electron density sufficient to allow the self-focusing process to happen and shrink the laser beam.

An estimation of the spot diameter on the target surface due to self-focusing process occurring at $FP = -200\ \mu m$ was given taking into account Eq. (3) indicating that the spot area is inversely proportional to the laser intensity. Assuming, as a first approximation, that the maximum

https://doi.org/10.1017/S0263034608000396 Published online by Cambridge University Press

charge state increases linearly with the laser intensity, in agreement with literature data (Laska *et al.*, 2005*b*, 2007), the maximum charge increment from Au^{44+} up to Au^{56+}, can be correlated to an increment of the laser intensity. Because the ionization potential of Au^{44+} and Au^{56+} are $I_1 = 1.834$ keV and $I_2 = 3.395$ keV, respectively, the spot diameters D_2 and D_1, in the presence of self-focusing and not-self-focusing effects, respectively, can be correlated to the ionization potentials through the expression:

$$D_2 = D_1 \cdot \sqrt{\frac{I_1}{I_2}} = 51\ \mu m \tag{5}$$

indicating that a 72% reduction of the laser spot diameter occurs during the self-focusing effect.

The insets in Figure 7 report the typical IEA spectra obtained in the two cases of non-self-focusing (a) and self-focusing occurrence (b).

The self-focusing electron density threshold (n_e) may be calculated by Eqs (1) and (2). In our experimental conditions, the laser frequency ω_L is 4.3×10^{15} rad/s, which corresponds to a laser power and a critical density of 5×10^{11} W and 5.8×10^{22} electrons/cm^3, respectively. Thus the corresponding electron density threshold is 1.88×10^{21} electrons/cm^3.

Assuming, during self-focusing effect, to have a mean charge state of 28+, this means that the maximum atom density should be 6.7×10^{19} atoms/cm^3. These atoms can be represented inside a plasma lens having an approximated volume of the order of 6.5×10^{-7} cm^3 (230 μm length and 60 μm diameter).

Experimental results demonstrated that this volume represents only a small part (less than 10%) of the final crater volume created by the laser pulse on the Au target.

ACKNOWLEDGEMENT

This work was partly supported by the Grant Agency of the ASCR (Grant IAA100100715).

REFERENCES

Batani, D., Dezulian, R., Redaelli, R., Benocci, R., Stabile, H., Canova, F., Desai, T., Lucchini, G., Krousky, E., Masek, K., Pfeifer, M., Skala, J., Dudzak, R., Rus, B., Ullschmied, J., Malka, V., Faure, J., Koenig, M., Limpouch, J., Nazarov, W., Pepler, D., Nagai, K., Norimatsu, T. & Nishimura, H. (2007). Recent experiments on the hydrodynamics of laser-produced plasmas conducted at the PALS laboratory. *Laser Part. Beams* **25**, 127–141.

Bell, A.R. (1996). Laser-produced plasma. In *Plasma Physics and Introduction Course* (Dendy R., ed.). New York: Cambridge University Press.

Giulietti, D. & Gizzi, L.A. (1998). X-ray emission from-laser-produced plasmas. *Rivista Nuovo Cimento* **21**, 1–93.

Giulietti, A., Galimberti, M., Gamucci, A., Giulietti, D., Gizzi, L.A., Koester, P., Labate, L., Tomassini, P., Ceccotti, T., D'Oliveira, P., Auguste, T., Monot, P. & Martin, P. (2007). Search for stable propagation of intense femtosecond laser pulses in gas. *Laser Part. Beams* **25**, 513–521.

Jungwirth, K. (2005). Recent highlights of the PALS research program. *Laser Part. Beams* **23**, 177–182.

Koyama, K., Adachi, M., Miura, E., Kato, S., Masuda, S., Watanabe, T., Ogata, A. & Tanimoto, M. (2006). Monoenergetic electron beam generation from a laser-plasma accelerator. *Laser Part. Beams* **24**, 95–100.

Laska, L., Badziak, J., Gammino, S., Jungwirth, K., Kasperczuk, A., Krasa, J., Krousky, E., Kubes, P., Parys, P., Pfeifer, M., Pisarczyk, T., Rohlena, K., Rosinski, M., Ryc, L., Skala, J., Torrisi, L., Ullschmied, J., Velyhan, A. & Wolowsk, J. (2007). The influence of an intense laser beam interaction with preformed plasma on the characteristics of emitted ion streams. *Laser Part. Beams* **25**, 549–556.

Laska, L., Jungwirth, K., Kralikova, B., Krasa, J., Krousky, E., Masek, K., Pfeifer, M., Rohlena, K., Skala, J., Ullschmied, J., Badziak, J., Parys, P., Ryc, L., Szydlowski, A., Wolowski, J., Woryna, E., Ciavola, G., Gammino, S., Torrisi, L. & Boody, F.P. (2004). Review of laser ion sources developments in Prague and production of q over 50+ ions at Prague Asterix Laser System (Invited). *Rev. Sci. Instr.* **75**, 1546–1550.

Laska, L., Jungwirth, K., Krasa, J., Krousky, E., Pfeifer, M., Rohlena, K., Skala, J., Ullschmied, J., Velyhan, A., Kubes, P., Badziak, J., Parys, P., Rosinski, M., Ryc, L. & Wolowski, J. (2006*a*). Experimental studies of interaction of intense long laser pulse with a laser-created Ta plasma. *Czech J. Phys.* **56**, B506–B514.

Laska, L., Jungwirth, K., Krasa, J., Krousky, E., Pfeifer, M., Rohlena, K., Ullschmied, J. Badziak, J., Parys, P., Wolowski, J., Gammino, S., Torrisi, L. & Boody, F.P. (2006*b*). Self-focusing in processes of laser generation of highly-charged and high-energy heavy ions. *Laser Part. Beams* **24**, 175–179.

Laska, L., Jungwirth, K., Krasa, J., Pfeifer, M., Rohlena, K. & Ullschmied, J. (2005*a*). The effect of pre-plasma and self-focusing on characteristics of laser produced ions. *Czech. J. Phys.* **55**, 691–699.

Laska, L., Ryc, L., Badziak, J., Boody, F.P., Gammino, S., Jungwirth, K., Krasa, J., Krousky, E., Mezzasalma, A., Parys, P., Pfeifer, M., Rohlena, K., Torrisi, L., Ullschmied, J. & Wolowski, J. (2005*b*). Correlation of highly charged ion and X-ray emissions from the laser-produced plasma in the presence of non-linear phenomena. *Rad. Effects Defects Solids* **160**, 557–566.

Lifschitz, A.F., Faure, J., Glinec, Y., Malka, V. & Mora, P. (2006). Proposed scheme for compact GeV laser plasma accelerator. *Laser Part. Beams* **24**, 255–259.

Malka, V. & Fritzler, S. (2004). Electron and proton beams produced by ultra short laser pulses in the relativistic regime. *Laser Part. Beams* **22**, 399–405.

Malka, V., Faure, J., Glinec, Y. & Lifschitz, A.F. (2006). Laser-plasma accelerator: Status and perspectives. *Phil. Trans. R. Soc. A* **364**, 601.

Mangles, S.P.D., Walton, B.R., Najmudin, Z., Dangor, A.E., Krushelnick, K., Malka, V., Manclossi, M., Lopes, N., Carias, C., Mendes, G. & Dorchies, F. (2006). Table-top laser-plasma acceleration as an electron radiography source. *Laser PartT. Beams* **24**, 185–190.

Margarone, D., Laska, L., Torrisi, L., Gammino, S., Krasa, J., Krousky, E., Parys, P., Pfeifer, M., Rohlena, K., Rosinski,

M., Ryc, L., Skala, J., Ullschmied, J., Velyhan, A. (2007). Studies of craters' dimension for long-pulse laser ablation of metal targets at various experimental conditions. *Appl. Surf. Sci.* **254**, 2797–2803.

Sun, G.Z., Ott, E., Lee, Y.C. & Guzdar, P. (1987). Self-focusing of short intense pulses in plasmas. *Phys. Fluids* **30**, 526–532.

Torrisi, L., Gammino, S., Ando, L., Mezzasalma, A.M., Badziak, J., Parys, P., Wolowski, J., Woryna, E., Jungwirth, K., Kralikova, B., Krasa, J., Laska, L., Pfeifer, M., Rohlena, K., Skala, J., Ullschmied, J. & Boody, F.P. (2002). Study of the etching process and crater formation induced by intense laser pulses at PALS. *Czech. J. Phys.* **52**, 329–334.

Woryna, E., Parys, P., Wolowski, J. & Mroz, W. (1996). Corpuscular diagnostics and processing methods applied in investigations of laser-produced plasma as a source of highly ionized ions. *Laser Part. Beams* **14**, 293–321.